Electric field control of magnetic properties in FeRh/PMN-PT heterostructures

Yali Xie, Qingfeng Zhan, Tian Shang, Huali Yang, Yiwei Liu, Baomin Wang, and Run-Wei Li

Citation: AIP Advances **8**, 055816 (2018); doi: 10.1063/1.5003435
View online: https://doi.org/10.1063/1.5003435
View Table of Contents: http://aip.scitation.org/toc/adv/8/5
Published by the American Institute of Physics

Electric field control of magnetic properties in FeRh/PMN-PT heterostructures

Yali Xie, Qingfeng Zhan,[a] Tian Shang, Huali Yang, Yiwei Liu, Baomin Wang, and Run-Wei Li[a]

CAS Key Laboratory of Magnetic Materials and Devices & Zhejiang Province Key Laboratory of Magnetic Materials and Application Technology, Ningbo Institute of Material Technology and Engineering, Chinese Academy of Sciences, Ningbo 315201, People's Republic of China

(Presented 7 November 2017; received 6 September 2017; accepted 14 November 2017; published online 3 January 2018)

We investigated electric control of magnetic properties in FeRh/PMN-PT heterostructures. An electric field of 1 kV/cm applied on the PMN-PT substrate could increase the coercivity of FeRh film from 60 to 161 Oe at 360 K where the FeRh antiferromagnetic to ferromagnetic phase transition occurs. The electric field dependent coercive field reveals a butterfly shape, indicating a strain-mediated magnetoelectric coupling across the FeRh/PMN-PT interface. However, the uniaxial magnetic anisotropy of FeRh is almost unchanged with the applied electric field on the PMN-PT substrate, which suggests the change of coercivity in FeRh films is mainly due to the shift of the magnetic transition temperature under the electric field.
https://doi.org/10.1063/1.5003435

The CsCl-type FeRh alloy is antiferromagnetic (AF) at room temperature. It undergoes a peculiar first-order phase transition to ferromagnetic (FM) phase upon heating above 300 K and shows two-phase coexistence near the transition.[1–3] Due to the magnetic transition, FeRh in the form of thin films have attracted extensive attentions for its potential application in the spintronic devices, especially in heat assisted magnetic recording.[4–9] However, the high energy cost of the thermally induced magnetic transition is detrimental to the practical application. In recent year, many attempts have been made to control the magnetic transition by other techniques such as electric field, magnetic field, mechanical strain, optical pulses, *etc*.[4,10–15] For instance, Suzuki *et al.* demonstrated an elastically induced FM to AF phase transition in Ga-substituted FeRh thin films on $BaTiO_3(001)$.[10] Ju *et al.* showed that the ultrafast generation of FM order can be achieved by driving FeRh from an AF to a FM state using femtosecond optical pulses.[11] Among these techniques, electric control of magnetism has been proved to be an effective way with low energy consumption to change the orientation of magnetic moment, magnetization, magnetic anisotropy, magnetic phase transition, and coercive field in FM/ferroelectric (FE) magnetoelectric laminate heterostructures.[16–20] For example, Xuan *et al.* showed that the magnetization changes about 7% with an applied electric field of 10 kV/cm on a Ni/PMN-PT/Ni composite.[19] Weiler *et al.* demonstrated that magnetic easy axis in the Ni film plane is rotated by 90° upon changing the polarity of the electric field applied to the $Pb(Zr_xTi_{1-x})O_3$ actuator in a Ni/$Pb(Zr_xTi_{1-x})O_3$ composite.[20] Subsequently, the studies on FeRh/FE heterostructures also generated great interest due to its applications in spintronics.[21–23] Lee *et al.* reported a 8% change in the electrical resistivity controlled by applying an electric field on FeRh/PMN-PT heterostructures.[22] Liu *et al.* report a giant, ~22%, electroresistance modulation for FeRh above room temperature by a small electric field of 2 kV/cm and the resulting magnetic phase transition in epitaxial FeRh/$BaTiO_3$ heterostructures.[23] These previous studies mostly focused on electrical transport behaviors of FeRh

[a]Electronic mail: zhanqf@nimte.ac.cn and runweili@nimte.ac.cn

thin films during the magnetic phase transition driven by electric field. In this work, we investigated the control of magnetic properties of FeRh films by applying electric field on the ferroelectric (1-x)[$Pb(Mg_{1/3}Nb_{2/3})O_3$]-x[$PbTiO_3$] (PMN-PT) substrates. The electric field dependent coercivity of FeRh films exhibits a symmetrical butterfly-type behavior, indicating a strain-mediated magnetoelectric coupling. The uniaxial magnetic anisotropy of FeRh films is almost unchanged when varying the electric field, suggesting the change of FeRh coercivity in films is mainly due to the shift of the magnetic transition temperature under the electric field.

FeRh thin films with a thickness of 30 nm were deposited on commercial (001)-oriented PMN-PT ferroelectric substrates in a magnetron sputtering system with a base pressure below 1.0×10^{-5} Pa. The substrates were annealed at 600 °C for 1 h in vacuum chamber and then held at 650 °C during deposition. After growth, FeRh films were annealed at 700 °C for 1 h. Prior to be taken out of the vacuum chamber, FeRh films were capped by a 3 nm Ta layer to avoid oxidation. The film thicknesses were controlled by the deposition time, which have been calibrated by X-ray reflectivity (XRR). The temperature dependence of magnetic behaviors of FeRh films were characterized by using a magneto-optical Kerr effect (MOKE) system and a magnetic properties measurement system (MPMS, Quantum Design). During the MOKE measurement, an external electric field was applied through the thickness of PMN-PT substrates, as schematically shown in Fig. 1(a).

Figure 1(b) plots the temperature dependent magnetization of FeRh film grown on PMN-PT measured with an in-plane magnetic field of 2 kOe. Due to the large lattice mismatch, FeRh films grown on PMN-PT display a polycrystalline behavior. At room temperature, the polycrystalline FeRh films are mostly in the AF order with a small magnetization about 190 emu/cm^3. The value is obviously larger than that of single crystal FeRh film epitaxial grown on MgO substrate. As the temperature increases, the magnetization steeply increases to 720 emu/cm^3 around 350 K, indicating a typical AF to FM phase transition. In contrast, the magnetization of FeRh film grown on MgO can reach as high as 1000 emu/cm^3 after the AF-FM phase transition. In the cooling process, the magnetization of FeRh films can be reversibly reduced to the original value of AF state. A temperature hysteresis of the magnetization about 50 K is revealed, indicating the first order phase transition of FeRh. The relatively high magnetization of FeRh below the critical temperature, the rather low magnetization above the critical temperature, and the reversible AF-FM phase transition likely suggest three kinds of magnetic phase in the polycrystalline FeRh including the irreversible FM phase, the irreversible AF phase, and the reversible AF-FM phase. Previous studies on FeRh thin films ascribed the high

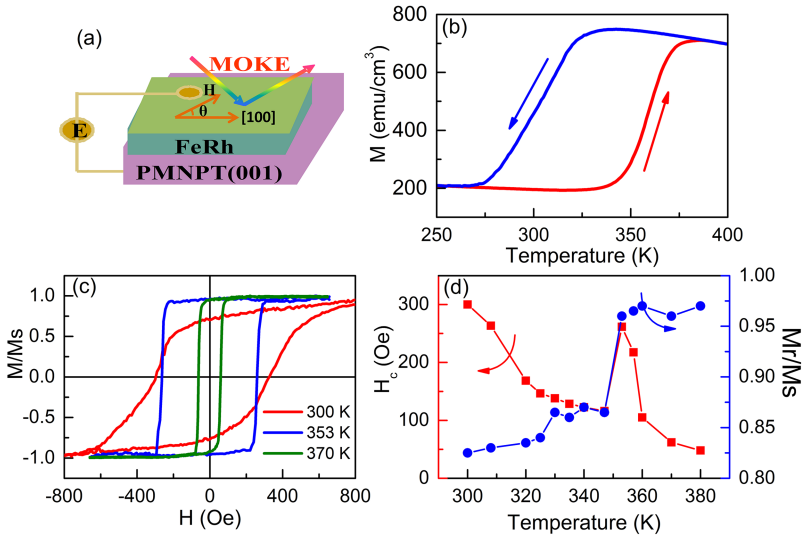

FIG. 1. (a) The sample structure and the measurement configuration. (b) The temperature dependent magnetization of FeRh/PMN-PT heterostructure measured with an applied field of 2 kOe. (c) The magnetic hysteresis loops of FeRh/PMN-PT heterostructure measured in the increasing branch of temperature. (d) The temperature dependent coercive field and remanence ratio of FeRh/PMN-PT heterostructure.

magnetization of the room-temperature AF state to the small fraction of the FM phase located at the grain boundary.[24] In our case, due to the polycrystalline structure, the induced FM phase is obviously enhanced, leading to a considerable magnetization at the room-temperature AF state. In addition, the rather low magnetization at the high-temperature FM state indicates the existence of the irreversible AF phase in polycrystalline FeRh films even beyond the AF-FM transition temperature.[25] This part of AF phase may located at the grain center and do not follow the AF-FM phase transition, but keep at the AF state even above the critical temperature.[26] Besides the irreversible FM and AF phases, the main part of reversible AF-FM phase responses for the reversible temperature dependent magnetic behaviors of polycrystalline FeRh film.

The Kerr hysteresis loops of FeRh/PMN-PT measured at different temperatures in the heating process are presented in Fig. 1(c). At room temperature, the FeRh thin film exhibits a slant hysteresis loop with a coercivity (H_c) of 302 Oe and a remanence ratio (M_r/M_s) of 0.8. The Kerr signal comes from the irreversible FM phase. Due to the pinning effect by the AF phase, the coercive field of the irreversible FM phase becomes obviously large. With increasing temperature to 353 K, H_c deceases to 262 Oe but the remanence ratio increases to 0.96. This is because the reversible AF phase starts to transfer to the FM phase when approaching to the AF-FM critical temperature, thus the reduced AF phase may lower the pinning effect exerting on the FM phase and reduce the coercivity. At 370 K, the reversible FeRh AF phases have changed to the FM phase. Consequently, H_c is further reduced to 60 Oe, and the remanence ratio is 0.96. Figure 1(d) displays the temperature dependence of H_c and M_r/M_s of FeRh thin films from 300 to 380 K in the heating process. Besides the decrease with temperature, the temperature dependence of H_c shows a local peak around the critical temperature of 350 K. In contrast, the M_r/M_s ratio shows a step-like increase at the critical temperature, reaching close to 1.0. The temperature dependent behaviors of FeRh films are similar to that observed in exchange biased FM/AF bilayer where H_c shows a peak at the blocking temperature due to a large fraction of the hysteretic losses occurring in the AF layer in the range of temperature. Similarly, in FeRh films the AF phase around the AF-FM transition temperature produces additional hysteretic losses to FM phase, giving rise to the enhanced coercivity.

Figures 2(a)–2(c) show the Kerr hysteresis loops of FeRh films measured in the heating process of temperature with an electric field ranged from -6 kV/cm to 6 kV/cm applied on the PMN-PT substrate.

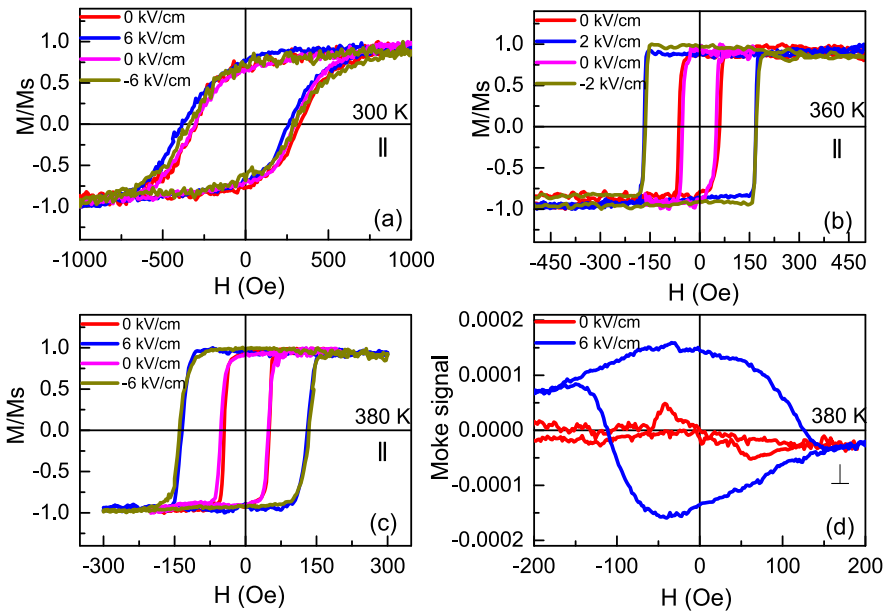

FIG. 2. Typical longitudinal (∥) MOKE loops of FeRh films measured in the increasing branch of temperature with different electric fields applied on the PMN-PT substrates at (a) 300 K, (b) 360 K, and (c) 380 K. (d) Typical transverse (⊥) MOKE loops of FeRh films measured with different electric fields applied on the PMN-PT substrates at 380 K.

Due to the large converse piezoelectric effect ($d_{33} \sim 2800$ pC/N),[27] an applied electric field of 6 kV/cm on PMN-PT can produce a biaxial compressive strain about 0.1% in the film plane.[22] As shown in Fig. 2(a), at room temperature before the occurrence of AF-FM phase transition, the longitudinal Kerr hysteresis loops keep almost unchanged regardless of the application of different electric fields. This observation indicates the magnetic properties of the irreversible FM phase in polycrystalline FeRh films are insensitive to the external strain, suggesting a neglectable inverse magnetostrictive effect in FeRh films. With increasing the temperature to 360 K, a part of reversible FeRh phase has been transferred from the AF to FM phases. In this case, the coercivity of FeRh film increases from 61 to 168 Oe when applying an electric field of 2 kV/cm on the PMN-PT substrate, as shown in Fig. 2(b). After removing the electric field, the hysteresis loop is almost recovered to the initial state. The slight difference in coercivity is likely due to the ferroelectric relaxation of PMN-PT. A negative electric field of -2 kV/cm leads to an identical change of FeRh hysteresis loop as comparison with the one with a positive electric field of 2 kV/cm. During the variation of electric field, the squareness of hysteresis loop is almost unchanged and keeps about 1.0. The change of coercivity upon applying electric field can be understood by the strain-driven magnetic phase transition. It is well known that the AF-FM transition of FeRh is accompanied by an expansion in the unit cell volume. When an electric field applied on the PMN-PT substrate, the induced biaxial compressive strain can suppress the lattice expansion of FeRh and thus increase the AF-FM phase transition temperature.[22] Thus, a part of FM phase is isothermally transferred to the AF phase. Consequently, the enhancement of the pinning effect by the increased AF phase may improve the coercivity of the FM phase in FeRh films. At 380 K, the reversible FeRh phase completely undergoes the AF-FM phase transition. The applied electric field reduces the critical temperature and drives the FM FeRh back to the AF-FM coexisting phase. Thus, the coercivity increases from 47 to 132 Oe due to the additional pinning effect by the AF phase when increasing the electric field to 6 kV/cm, as shown in Fig. 2(c). After removing the electric field, the hysteresis loop of FeRh film is quickly restored. The negative applied electric field could give rise to the same variation of magnetic properties of FeRh films as the positive one. It should be noted that due to the temperature hysteresis of magnetization, at a temperature between 275 and 375 K in the cooling branch, a part of reversible FM component is not changed to the AF state. Therefore, at the temperature range from 275 and 375 K, the FM component in the cooling branch is more than that in the heating branch, leading to slightly different magnetic behaviors.

In order to understand the magnetization reversal mechanism of FeRh films under different applied electric fields, we additionally measured the transverse Kerr hysteresis loops. At 380 K above the critical temperature, only a weak transverse Kerr signal was observed without applying electric field, indicating that the magnetization switches is dominated by the domain wall nucleation and propagation, as shown in Fig. 2(d). In contrast, after applying a 6 kV/cm electric field, an obvious transverse Kerr loop was revealed, suggesting the magnetization reversal mechanism has changed to the coherent rotation. At 300 K before the occurrence of AF-FM phase transition, whether the electric field is applied or not, the non-vanishing transverse loops indicate an in-plane rotation of magnetization. At 360 K where the AF to FM phase transition occurs, the transverse loops with and without applying electric field behave like that of 300K, indicating the magnetization reversal mechanism of in-plane rotation.

Figures 3(a)–3(c) summarize the coercivity of FeRh films as a function of the applied electric field at different temperatures. The symmetrical butterfly shape indicates a strain-mediated magnetoelectric coupling across the FeRh/PMN-PT interface. The difference is that the coercivity at 300 and 380 K increases gradually with the applied electric field. However, at 360 K, the coercivity of FeRh film is 60 Oe without applying electric field. It steeply increases to 161 Oe at 1.0 kV/cm, and reaches a saturation value of 169 Oe with further increasing the electric field. Our results indicate the most efficient electric control of magnetic properties in FeRh film should be operated at the AF-FM coexisting state around the phase transition temperature.

Obviously, both the change of magnetic anisotropy and the shift of phase transition temperature induced by applying electric field on the ferroelectric substrates may be responsible for the variation of the coercivity of FeRh films. In order to figure out this problem, we investigated the magnetic anisotropy of FeRh films by measuring the angular dependence of MOKE signal, which directly measures the magnetization projected in the optical incident plane. Figures 4(a) and 4(b) present

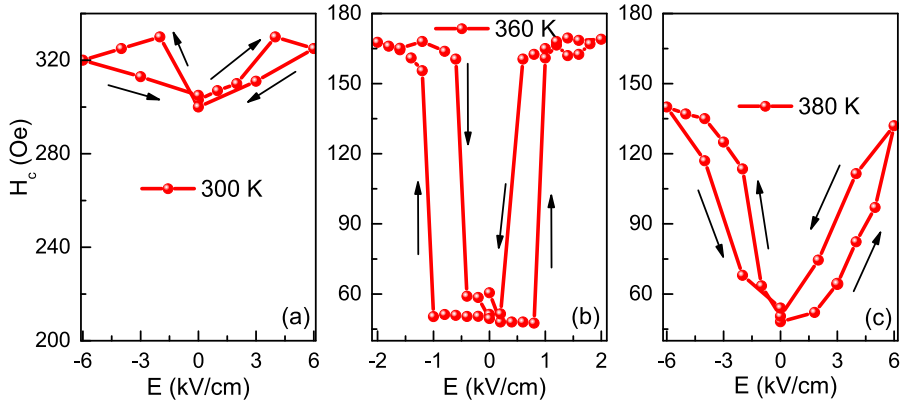

FIG. 3. The coercive field of FeRh films measured at different electric fields at (a) 300 K, (b) 360 K, and (c) 380 K.

the MOKE signal as a function of the field orientation θ at 300 K without electric field and with applying 4 kV/cm electric field, respectively. Regardless of the applied magnetic field, the angular dependent MOKE signal display a twofold symmetry, indicating a uniaxial magnetic anisotropy in FeRh film. The uniaxial magnetic anisotropy can be quantitatively obtained by fitting the angular dependence of MOKE signal measurement by analyzing the magnetic torque.[28] The fitting for the angular dependent MOKE signal indicates that the uniaxial magnetic anisotropy at 300 K keeps very weak before and after applying electric field. Figures 4(c) and 4(d) show the MOKE signal as a function of θ at 380 K without electric field and with applying 4 kV/cm electric field, respectively. The estimated uniaxial magnetic anisotropy slightly changes from 1.14×10^5 to 1.19×10^5 erg/cm^3 with increasing the electric field from 0 to 4 kV/cm, which indicates a rather small magnetostrictive constant of FeRh films. Therefore, we ascribe the variation of coercive fields of FeRh films under an applied electric field mainly due to the shift of phase transition temperature.

In summary, we have studied the electric field control of magnetic properties in FeRh/PMN-PT heterostructure. The as-prepared samples present a first-order magnetic phase transition from AF to FM orders at a critical temperature around 360 K. It was found that the electric field dependent

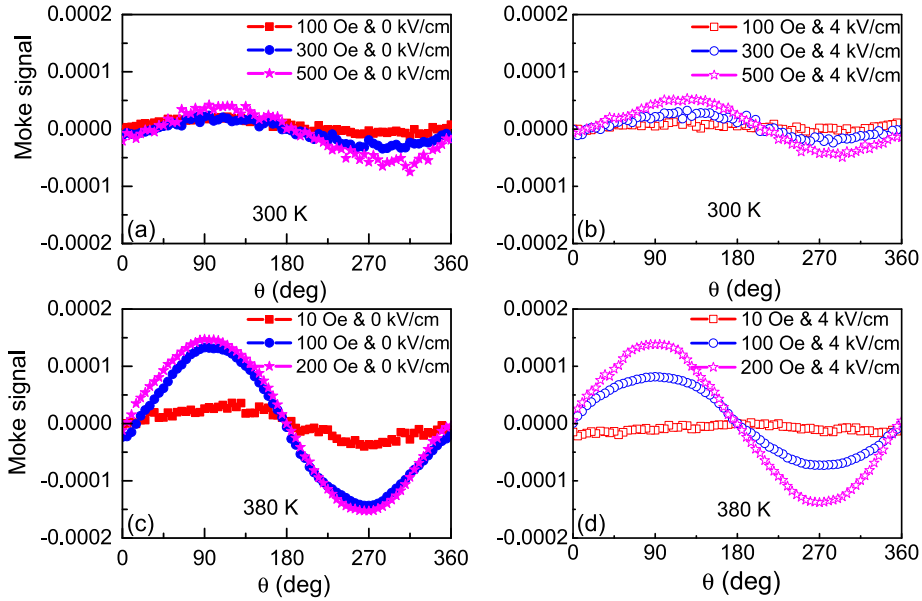

FIG. 4. The angular dependence of MOKE signal measured under different electric fields with different magnetic fields for FeRh/PMN-PT films. The measurement temperature is (a), (b) 300 K, (c), (d) 380 K.

coercivity of FeRh films shows a symmetrical butterfly-type behavior, indicating a strain-mediated magnetoelectric coupling. In addition, magnetic anisotropy of FeRh films is almost unchanged when varying the electric field, suggesting the change of FeRh coercivity in films is mainly due to the shift of the magnetic transition temperature under the electric field.

This work was financially supported by the National Natural Science Foundation of China (11404349, 11474295, 51522105, 51525103 and 51401230, 61774161), the Ningbo Science and Technology Innovation Team (2015B11001), the National Key R&D Program of China (2016YFA0201102) and Ningbo Natural Science Foundation (2015A610110, 2017A610093).

[1] M. Fallot, Ann. Phys. **10**, 291 (1938).
[2] J. S. Kouvel and C. C. Hartelius, J. Appl. Phys. **33**, 1343 (1962).
[3] A. I. Zakharov, A. M. Kadomtseva, R. Z. Levitin, and E. G. Ponyatovskii, Sov. Phys. JETP **19**, 1348 (1964).
[4] S. Maat, J.-U. Thiele, and E. E. Fullerton, Phys. Rev. B **72**, 214432 (2005).
[5] C. Stamm, J.-U. Thiele, T. Kachel, I. Radu, P. Ramm, M. Kosuth, J. Minár, H. Ebert, H. A. Dürr, W. Eberhardt, and C. H. Back, Phys. Rev. B **77**, 184401 (2008).
[6] M. Sharma, H. M. Aarbogh, J. U. Thiele, S. Maat, E. E. Fullerton, and C. Leighton, J. Appl. Phys. **109**, 083913 (2011).
[7] M. A. de Vries, M. Loving, A. P. Mihai, L. H. Lewis, D. Heiman, and C. H. Marrows, New J. Phys. **15**, 013008 (2013).
[8] C. Bordel, J. Juraszek, D. W. Cooke, C. Baldasseroni, S. Mankovsky, J. Minár, H. Ebert, S. Moyerman, E. E. Fullerton, and F. Hellman, Phys. Rev. Lett. **109**, 117201 (2012).
[9] J.-U. Thiele, S. Maat, and E. E. Fullerton, Appl. Phys. Lett. **82**, 2859 (2003).
[10] I. Suzuki, M. Itoh, and T. Taniyama, Appl. Phys. Lett. **104**, 022401 (2014).
[11] G. Ju, J. Hohlfeld, B. Bergman, R. J. M. van deVeerdonk, O. N. Mryasov, J.-Y. Kim, X. Wu, D. Weller, and B. Koopmans, Phys. Rev. Lett. **93**, 197403 (2004).
[12] G. Shirane, C. W. Chen, P. A. Flinn, and R. Nathans, Phys. Rev. **131**, 183 (1963).
[13] P. H. L. Walter, J. Appl. Phys. **35**, 938 (1964).
[14] C. J. Schinkel, R. Hartog, and F. H. A. M. Hochstenbach, J. Phys. F Met. Phys. **4**, 1412 (1974).
[15] R. Barua, F. Jiménez-Villacorta, and L. H. Lewis, Appl. Phys. Lett. **103**, 102407 (2013).
[16] M. Weisheit, S. Fähler, A. Marty, Y. Souche, C. Poinsignon, and D. Givord, Science **315**, 349 (2007).
[17] S. Brivio, D. Petti, R. Bertacco, and J. C. Cezar, Appl. Phys. Lett. **98**, 102506 (2011).
[18] Z. G. Wang, Y. D. Yang, R. Viswan, J. F. Li, and D. Viehland, Appl. Phys. Lett. **99**, 043110 (2011).
[19] H. C. Xuan, L. Y. Wang, Y. X. Zheng, Y. L. Li, Q. Q. Cao, S. Y. Chen, D. H. Wang, Z. G. Huang, and Y. W. Du, Appl. Phys. Lett. **99**, 032509 (2011).
[20] M. Weiler, A. Brandlmaier, S. Geprägs, M. Althammer, M. Opel, C. Bihler, H. Huebl, M. S. Brandt, R. Gross, and S. T. B. Goennenwein, New J. Phys. **11**, 013021 (2009).
[21] R. O. Cherifi, V. Ivanovskaya, L. C. Phillips, A. Zobelli, I. C. Infante, E. Jacquet, V. Garcia, S. Fusil, P. R. Briddon, N. Guiblin, A. Mougin, A. A. Ünal, F. Kronast, S. Valencia, B. Dkhil, A. Barthélémy, and M. Bibes, Nat. Mater. **13**, 345 (2014).
[22] Y. Lee, Z. Q. Liu, J. T. Heron, J. D. Clarkson, J. Hong, C. Ko, M. D. Biegalski, U. Aschauer, S. L. Hsu, M. E. Nowakowski, J. Wu, H. M. Christen, S. Salahuddin, J. B. Bokor, N. A. Spaldin, D. G. Schlom, and R. Ramesh, Nat. Commun. **6**, 5959 (2015).
[23] Z. Q. Liu, L. Li, Z. Gai, J. D. Clarkson, S. L. Hsu, A. T. Wong, L. S. Fan, M.-W. Lin, C. M. Rouleau, T. Z. Ward, H. N. Lee, A. S. Sefat, H. M. Christen, and R. Ramesh, Phys. Rev. Lett. **116**, 097203 (2016).
[24] G. C. Han, J. J. Qiu, Q. J. Yap, P. Luo, T. Kanbe, T. Shige, D. E. Laughlin, and J. G. Zhu, J. Appl. Phys. **113**, 123909 (2013).
[25] Q. J. Yap, J. J. Qiu, P. Luo, J. F. Ying, G. C. Han, D. E. Laughlin, J.-G. Zhu, T. Kanbe, and T. Shige, J. Appl. Phys. **116**, 043902 (2014).
[26] M. Loving, F. Jimenez-Villacorta, B. Kaeswurm, D. A. Arena, C. H. Marrows, and L. H. Lewis, J. Phys. D: Appl. Phys. **46**, 162002 (2013).
[27] R. Zhang, B. Jiang, and W. W. Cao, Appl. Phys. Lett. **82**, 787 (2003).
[28] J. Li, E. Jin, H. Son, A. Tan, W. N. Cao, C. Hwang, and Z. Q. Qiu, Review of Scientific Instruments **83**, 033906 (2012).